Engineering Structures 54 (2013) 112–130

Contents lists available at SciVerse ScienceDirect

Engineering Structures

journal homepage: www.elsevier.com/locate/engstruct

# Experimental tests of different types of bolted steel beam–column joints under a central-column-removal scenario

Bo Yang [a,b,*], Kang Hai Tan [b]

[a] College of Civil Engineering, Chongqing University, Chongqing 400044, China
[b] School of Civil and Environmental Engineering, Nanyang Technological University, 50 Nanyang Avenue, 639798 Singapore, Singapore

ARTICLE INFO

*Article history:*
Received 19 December 2011
Revised 22 March 2013
Accepted 25 March 2013
Available online 11 May 2013

*Keywords:*
Progressive collapse
Connection
Beam–column joints
Catenary action
Large deformation
Experimental tests
Steel

ABSTRACT

Several structural collapse incidents indicate that failure usually started from beam–column joints when exposed to abnormal loads. If the connections are sufficiently robust and there is adequate axial restraint from adjoining structures, catenary action usually forms and gives rise to alternate load paths when affected columns are severely damaged, resulting in large deformations in adjoining beams and slabs. This paper presents seven experimental tests of the performance of common types of bolted steel beam–column joints under a central-column-removal scenario. The joint types including web cleat, top and seat angle, top and seat with web angle (TSWA) (8 mm angle), fin plate, flush end plate, extended end plate and TSWA(12 mm angle) are studied under the central-column-removal scenario. This study provides the behaviour and failure modes of different connections, including their abilities to deform in catenary mode. The test results indicate that the web cleat connection has the best performance in the development of catenary action, and the flush end plate, fin plate and TSWA connections could also deform in a ductile manner and develop catenary action prior to failure. It is worthy to note that tensile capacities of beam–column joints after undergoing large rotations usually control the failure mode and the formation of catenary action. A new tying resistance expression is proposed to consider the effect of large rotation. If large rotation is not considered in the design stage, the joints with poor rotation capacities would fail to achieve the design tying resistances. The test results also demonstrate that the rotation capacities of beam–column joints based on the experimental results in this study were much higher than the recommended values.

© 2013 Elsevier Ltd. All rights reserved.

## 1. Introduction

After the partial collapse of the Ronan Point apartment tower in 1968, engineers began to realise the importance of structural resistance to progressive collapse. More and more research works and design efforts are directed to this area, especially after the World Trade Centre disaster on 11 September 2001. The alternate load path method, an important design approach to mitigate progressive collapse, has been included by a number of design codes including GSA [1] and DoD [2]. This approach allows local failure to occur when subjected to an extreme load, but seeks to provide alternate load paths so that the initial damage can be contained and major collapse can be averted. A typical example is shown in Fig. 1 under the scenario when an interior column has been removed by blast and an alternate load path can take place through adjacent structural assemblage including beams, columns and joints. One of the key mechanisms to mitigate the spread of "domino" effect is to redistribute the applied load on damaged members through catenary action. As shown in Fig. 1, the term "catenary action" refers to the ability of beams to resist vertical loads through the formation of a string-like mechanism.

It is noteworthy that the beam–column joints are critical elements of any building structure and they usually control the extent of catenary action because of the limited resistance and rotation capacity of joints. However, although there have been extensive research studies on different types of joint behaviour under *gravity loads*, which have led to the codification of component-based approach to joint design [3], to date, there are relatively very few research studies of the joint behaviour when subjected to *abnormal loads*, especially for bolted steel connections.

Following the World Trade Centre disaster, some researchers have identified joint integrity as a key parameter to maintaining structural integrity under catenary action and have conducted extensive research works. Khandelwal and El-Tawil [4] carried out structural simulations to investigate a number of key design variables that influence the formation of catenary action in special steel moment-resisting frame sub-assemblages. Welded joints with and without reduced steel beam sections were considered. Sadek et al. [5] conducted an experimental and analytical assessment of the performance of steel beam–column assemblies with two types of moment-resisting connections similar to the ones

* Corresponding author. Tel.: +65 67904151.
*E-mail address:* yang0206@e.ntu.edu.sg (B. Yang).

0141-0296/$ - see front matter © 2013 Elsevier Ltd. All rights reserved.
http://dx.doi.org/10.1016/j.engstruct.2013.03.037

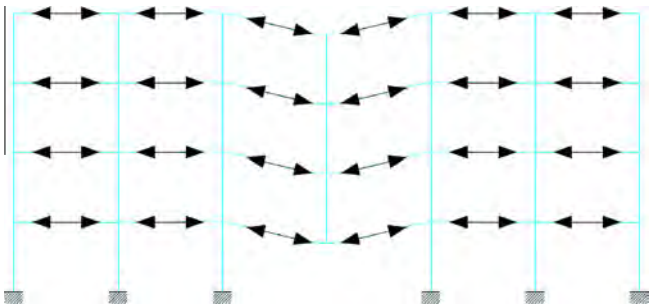

**Fig. 1.** Typical example of alternate load path.

investigated by Khandelwal and El-Tawil [4] under a middle column-removal scenario. In 2009, Karns et al. [6] conducted a test programme consisting of a steel frame subjected to blast. The behaviour of different beam–column joints subjected to blast was evaluated experimentally and numerically. Conventional welded moment and side-plate moment connections were investigated. Demonceau [7] conducted a substructure experimental test and five beam–column joint tests in order to observe the development of catenary action and its effect on the joint behaviour. The *M–N* interaction curves of composite joints (under hogging and sagging moments) were included in his work [7]. Izzuddin et al. [8] and Vlassis et al. [9] proposed a novel simplified framework for progressive collapse assessment of multi-storey buildings, considering sudden column loss as a design scenario. Other research works about progressive collapse can be found in Qian and Li [10], Sun et al. [11], Khandelwal and El-Tawil [12], Xu and Ellingwood [13] and Bao and Kunnath [14].

Ding and Wang [15], Dai et al. [16], Elsawaf et al. [17] and Wang et al. [18] conducted experimental tests and numerical simulations of structural fire behaviour of steel beam to column assemblies using different types of joints. Wang [19] presented a review of some recent research studies on steel joint behaviour under fire conditions. Yu et al. [20–23] conducted a series of experimental tests to investigate the robustness of common types of steel connections when subjected to fire. Fin plate, flexible end plate, flush end plate and web cleat connections were tested under fire conditions.

So far, only very limited research works have been conducted on bolted steel connections subjected to catenary action under column-removal scenarios. Most of the reported works focus on welded moment connections [4–6]. However, in Europe, bolted steel connections such as fin plate, flush end plate, web cleat and extended end plate, are very popular and the evaluation of these kinds of joints subjected to catenary action is important and timely. The behaviour of both simple and semi-rigid bolted steel connections under column-removal scenarios, in which the connections are subjected to monotonically increasing combined bending and tension, have not been experimentally investigated. The structures group at Nanyang Technological University is conducting a series of research programme to investigate the behaviour of steel and concrete structures under a middle column-removal scenario [24–26]. This project involves a series of tests on conventional simple and semi-rigid bolted steel connections, finite element (FE) investigation of connection behaviour, and development of mechanical models for analysis and design purpose. Yang and Tan [24] carried out the numerical simulations of the experimental tests, which are presented in the current paper. In addition, an extensive parametric study was undertaken using these validated numerical models to obtain the rotation capacities of various types of connections under catenary action. The current paper will only focus on the experimental tests of different types of steel bolted beam–column joints subjected to catenary action under a middle column-removal scenario and the design implications.

In total, seven experimental tests have been carried out on different types of steel beam–column joints, including simple and semi-rigid connections, at the Protective Engineering Laboratory of Nanyang Technological University. In the group of simple connections, web cleat, top and seat angle, top and seat with web angle (TSWA) (8 mm thickness angles) and fin plate connections were investigated while flush end plate, extended end plate and TSWA (12 mm thickness angles) constituted the group of semi-rigid connections. The principal aim of this paper is to provide the experimental results of bolted steel beam–column joint behaviour, including failure modes, development of forces and deflections in the beams under a middle column-removal scenario. The experimental results could be used to validate the numerical models. In addition, the robustness of different types of connections will also be assessed.

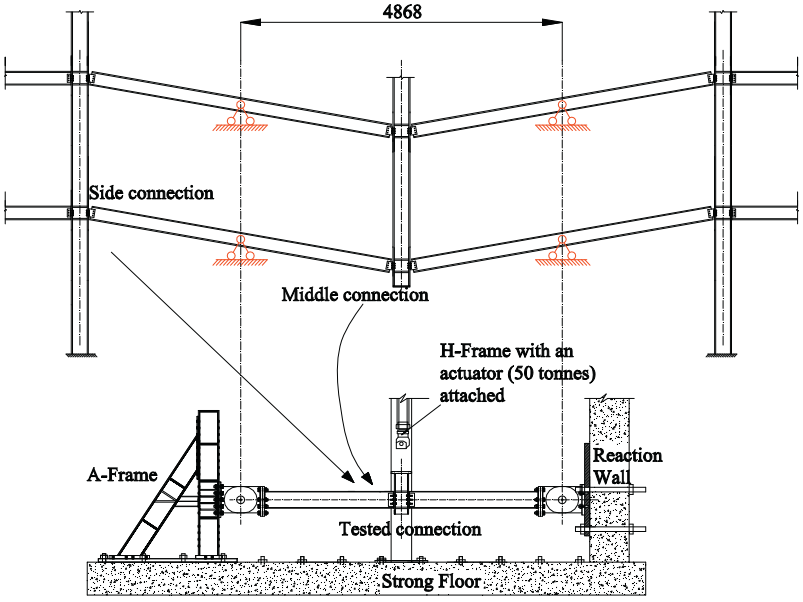


**Fig. 2.** Prototype beam–column joint.

## 2. Test set-up and specimens

### 2.1. Test set-up

The hypothetical beam–column joint considered for experimental tests is located above the storey where an internal column has been forcibly removed. As shown in Fig. 2, after the removal of the middle column, the internal forces and deflection of the middle and end connections are anti-symmetric. Thus, the inflection point locates at the middle of the beam span during the deflection process. Therefore, only half of the beam span is simulated using pin conditions, as shown in Fig. 2. The behaviour of the middle and end connections, including load-carrying and rotation capacities, could be represented by the tested specimens. A numerical simulation conducted by the authors demonstrates that the simplified test could provide equivalent performance to a sub-frame test. Although the vertical deflection capacities of the simplified and sub-frame tests are different, the rotation angles and internal forces experienced by the connections are identical. The simplified specimen is representative of any other upper floors above the zone of damage, since the whole column experiences a downward rigid body displacement and the axial forces in the column above the damaged storey are very small indeed and can be neglected.

It should also be noted that if the contribution of slabs is considered, the internal forces and deflection of the middle and end connections will be different. Nevertheless, the objectives of the current research work are to compare the performance of different types of connections and to validate numerical and component models. The relative performance of different types of connections will still be valid. The validated numerical and component models could be used in the sub-frame simulations. The slab effect will be studied in following works.

The test set-up is shown in Fig. 3. Horizontal restraint was provided by an A-frame and a strong reaction wall to consider the re-

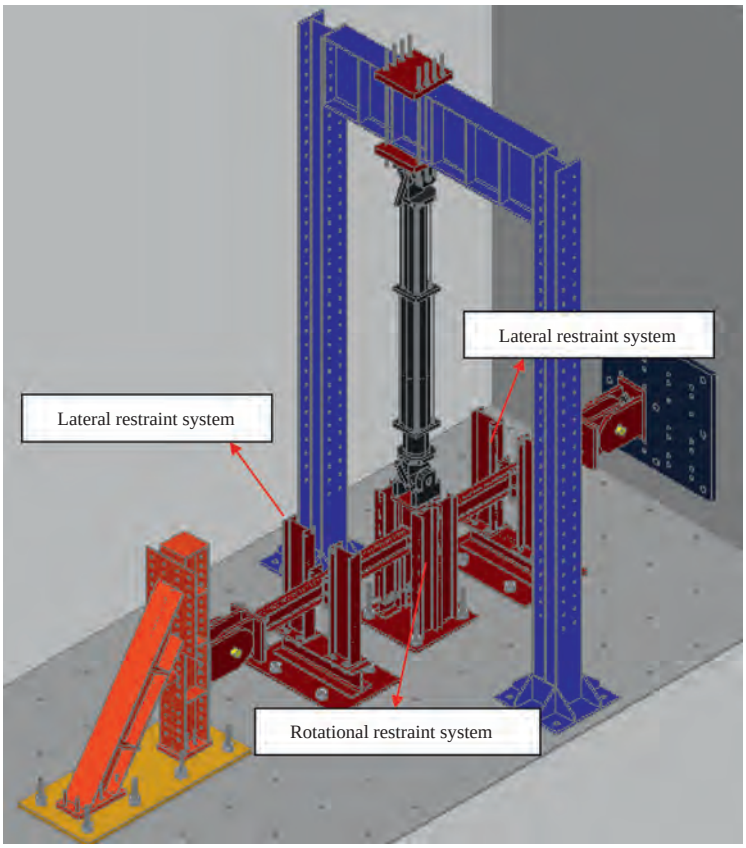


(a) Aerial view

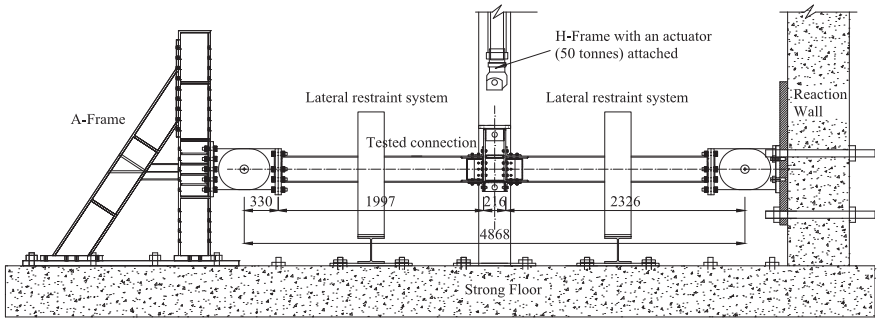


(b) Elevation view

**Fig. 3.** Test set-up (unit: mm).

(a) Rotational restraint system

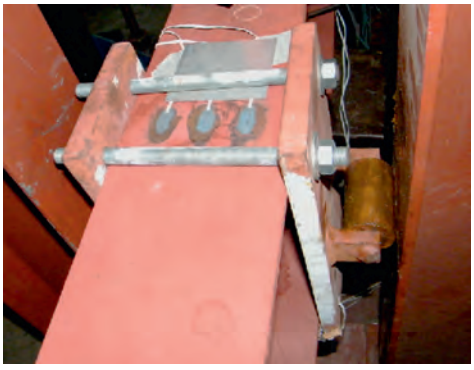

(b) Lateral restraint system

**Fig. 4.** Rotational and lateral restraint systems.

straint from surrounding structural elements. In order to consider the rotational restraint to beam–column joints from the continuous column of upper storeys, the test rig included a rotational restraint system at mid-span, as shown in Figs. 3 and 4. The column rotation was restrained by two steel rods, which would bear against the flanges of two steel columns during testing. In addition, the beams were restrained from lateral movement by two lateral restraint systems, as shown in Figs. 3 and 4. A displacement-controlled point load was applied to the middle column using an actuator, which was attached to a strong H-frame. Load was applied under displacement control at a rate of 6 mm/min.

### 2.2. Instrumentation

Measurements of internal forces were based on strain gauge measurements at four sections of steel beams, as shown in Fig. 5. The beam axial forces were estimated based on the measured strains across the beam section. Rosette strain gauges were attached onto the beam web to measure shear strains, so as to estimate the internal shear forces of beams. Actuator load was also measured by an external load cell so as to verify the external and internal forces in the test assembly.

The instrumentation included linear variable differential transducers (LVDTs) and line transducers for vertical deflection and joint rotation measurements. Ten LVDTs and four line transducers were placed in each specimen as shown in Fig. 6. One pair of LVDTs was placed horizontally at each side of the middle beam–column joint to capture the joint rotation. The remaining LVDTs and line transducers were placed along the beam length to measure in-plane vertical deflections.

### 2.3. Test specimens

A prototype steel framed building was designed for the purpose of examining its resistance against progressive collapse under column-removal scenarios. The multi-story office building had a plan dimension of 45 m by 30 m and a bracing system to resist lateral loads. Simple and semi-rigid beam–column joints were planned to study the effectiveness of different connection details in resisting progressive collapse under predominantly gravity load based on EC1:1.1 [27]. The dead loads and live loads for a typical bay of the building consisted of 5.1 kN/m$^2$ and 3 kN/m$^2$, respectively. The design standards of members and their connections were in accordance to EC3:1.1 [28], EC3:1.1 [29] and some UK design recommendations [30–32]. The highlighted area in Fig. 7 indicates a sub-assemblage of beams and connections that is typical of the

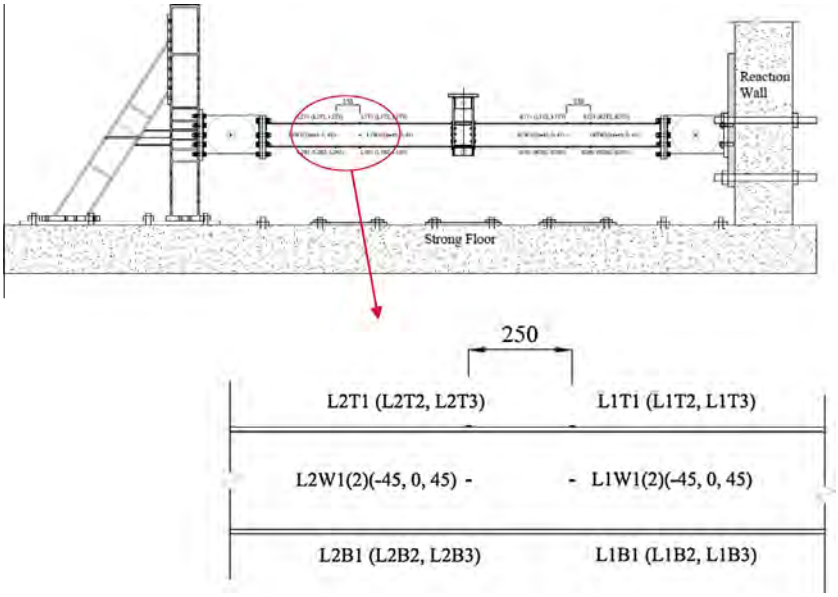


**Fig. 5.** Locations of strain gauges on test specimen (unit: mm).

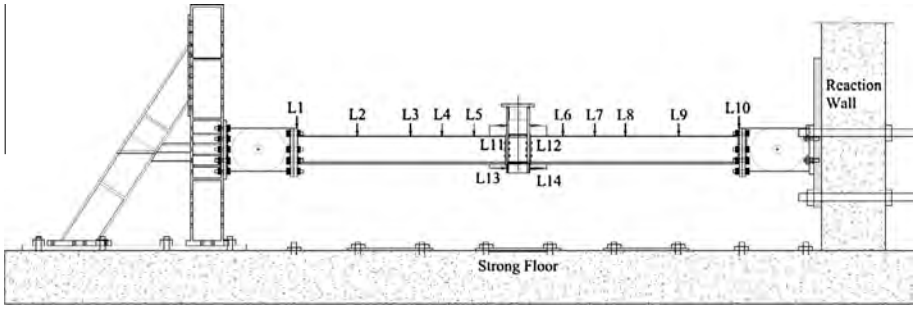


**Fig. 6.** Locations of LVDTs and line transducers on test specimen.

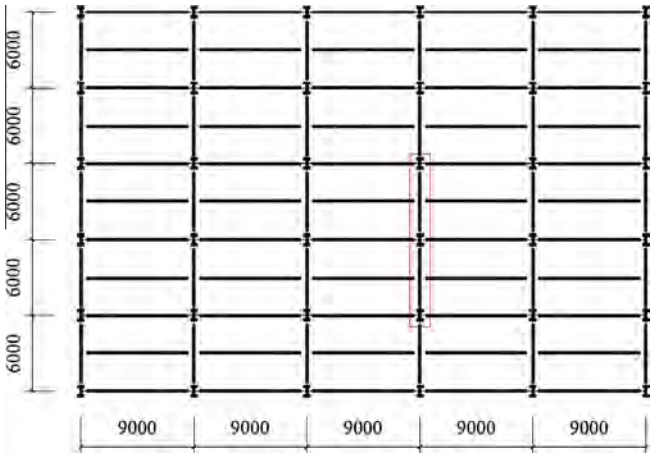


**Fig. 7.** Plan layout of the designed multi-story office building (unit: mm).

experimental tests reported herein. In the test programme, there were two series of specimens, viz. simple and semi-rigid bare steel beam–column joints and composite steel joints with profiled decking. Due to space limitation in the laboratory, the test specimens were scaled down to 2/3 of their original size. This paper only reports the behaviour of simple and semi-rigid bare steel joints subjected to catenary action.

Seven tests were carried out as shown in Table 1. Shear resistances and tying capacities, which were calculated based on UK design recommendations [30,31], are also listed in Table 1. For semi-rigid connections, moment resistance values were included as well. For both simple and semi-rigid jointed frames, the two-dimensional linear elastic analysis of one slice of the building in Fig. 7 was carried out. Only gravity load case was considered. In the design of simple connection specimens, beams were treated as simply-supported and beam–column joints could only transfer shear forces. However in the design of semi-rigid connection specimens, beams were treated as partial-continuous and beam–column joints could transfer shear forces as well as moments. Therefore, in the group of simple connection specimens, a deeper beam section of UB305 × 165 × 40 was used while in the group of semi-rigid connection specimens, the beam section changed to be UB254 × 146 × 37.

All specimens have the same length of 4208 mm with the distance between two pin supports as 4868 mm. Fig. 8 shows the construction details of the seven test specimens. Each specimen consisted of two steel beams and a steel column. The column cross-section in all the tests was the same, viz. Grade S355 UC203 × 203 × 71. In all the specimens, the beams and columns were strengthened by some stiffeners or welded thick plates to limit the influence of beam and column deformations on the connection behaviour. As shown in Fig. 8, four types of joints were investigated in the simple connections: web cleat, top and seat angle, TSWA (8 mm angle) and fin plate, while in the group of semi-rigid connections, three types of connection were studied: flush end plate, extended end plate and TSWA (12 mm angle). The specimen of TSWA (8 mm angle) has a relatively low flexural stiffness, which is smaller than $2EI/L$, where $L$ and $EI$ are the length and bending rigidity, respectively, of the steel beam. According to AISC [33], this specimen should be treated as simple connections. However, the specimen of TSWA (12 mm angle) has a higher flexural stiffness, which is greater than $2EI/L$ and smaller than $20EI/L$. According to AISC [33], it was treated as a semi-rigid connection (partially restrained connection). In all the tests the steel material of columns and beams was of grade S355 whereas the steel material of angles and welded plates was S275. Grade 8.8 M20 bolts were used for all specimens.

## 3. Test results

A summary of the test results is found in Table 2, from which the maximum vertical loads, the corresponding middle column displacement and rotation angles at the ends are given. The maximum horizontal reaction forces, the maximum moments and axial forces of beams and the failure modes are also included in this table. It should be mentioned that the rotation capacities of joints correspond to the maximum loads and these rotation angles are obtained by dividing the centre column displacement at the maximum load by the beam span of 2.326 m. This simplification is reasonable because plastic hinges are formed in the beam–column joints and the beam deflection profiles can be approximated by straight lines, as shown in Figs. 11, 21 and 25. In subsequent sections, the experimental results and observations from the seven connection tests, summarised in Table 2, are presented.

### 3.1. Simple connections

#### 3.1.1. Specimen 1—web cleat

The specimen was held at horizontal position, and a vertical load was gradually applied to the middle column. As the connection had limited capacity to resist moment, the specimen rotated at both ends with increasing deflection at the mid-span. Catenary action soon developed until fracture occurred in the central connection. Fig. 9 shows the vertical force–middle column displacement relationship for Specimen 1. At the initial loading stage, it could not resist any load until axial tensile force was mobilised in the beam due to large deflection, which marks the beginning of catenary action. As shown in Fig. 9, the load resisted by flexural action is quite limited. During the whole loading process, most of the load applied was resisted by catenary action. At a displacement of 367 mm, one of the web angles fractured close to the heel, which was immediately followed by the fracture of the other web angle. Fig. 10 shows the failure mode of the web cleat connection. Two

**Table 1**
Summary of test specimens.

| Specimen ID | Connection type | | Beam section | Column section | Bolt | End plate/angle | Shear/moment resistance[a] | Tying capacity[a] (kN) |
|---|---|---|---|---|---|---|---|---|
| Specimen 1 | Simple connections | Web cleat | 305 × 165 × 40 UB S355 | 203 × 203 × 71 UC S355 | Grade 8.8 M20 | l90 × 8 S275 | Shear: 124 kN | 177 |
| Specimen 2 | | Top and seat angle | 305 × 165 × 40 UB S355 | 203 × 203 × 71 UC S355 | Grade 8.8 M20 | l90 × 8 S275 | Shear: 152 kN | 153 |
| Specimen 3 | | TSWA (8 mm angle) | 305 × 165 × 40 UB S355 | 203 × 203 × 71 UC S355 | Grade 8.8 M20 | l90 × 8 S275 | Shear: 276 kN | 330 |
| Specimen 4 | | Fin plate | 305 × 165 × 40 UB S355 | 203 × 203 × 71 UC S355 | Grade 8.8 M20 | 100 × 8 S275 | Shear: 124 kN | 198 |
| Specimen 5 | Semi-rigid connections | Flush end plate | 254 × 146 × 37 UB S355 | 203 × 203 × 71 UC S355 | Grade 8.8 M20 | 200 × 12 S275 | *M*: 53 kN m, *S*: 332 kN | 480 |
| Specimen 6 | | Extended end plate | 254 × 146 × 37 UB S355 | 203 × 203 × 71 UC S355 | Grade 8.8 M20 | 200 × 12 S275 | *M*: 76 kN m, *S*: 516 kN | 546 |
| Specimen 7 | | TSWA (12 mm angle) | 254 × 146 × 37 UB S355 | 203 × 203 × 71 UC S355 | Grade 8.8 M20 | l150 × 90 × 12 S275 | *M*: 48 kN m, *S*: 480 kN | 495 |

[a] Design values obtained from Eurocode 3 [3] and BCSA/SCI [30,31].

observations are evident from the failure modes and action–vertical deformation curves: (1) catenary action formed prior to failure in the web cleat connection and (2) the beam segments remained straight and localized large strain occurred at the connection. As shown in Fig. 10c, the web angle experienced large deformation and localized yielding before fracture took place.

### 3.1.2. Specimen 2—top and seat angle

Significant flexural action is observed in Fig. 11 and the fracture mode of angles is similar with the web cleat test, as shown in Fig. 12. Top and seat angle connections are usually designed as simple connections. In conventional design, the top angle provides lateral support to the compression flange of the connecting beam, and the seat angle can only transfer vertical reaction of the beam to the column with minimal moment. However, this connection was able to transfer not only vertical reaction but also some end moment of the beam to the column. Fig. 11 shows the force–displacement relationship for Specimen 2. At the initial loading stage, applied load did not increase linearly. This is because when shear force exceeded friction forces in the tightened bolts between the adjoining beam bottom flange and the seat angle, the bolts loosened and slipped. After yielding of the bottom angles, the stiffness of the connection increased again due to plastic deformation of seat angles. As shown in Fig. 11b, at this stage, since the beam ends were horizontally restrained, the beams were in compression and bending. Fig. 11c shows that significant moment formed in the joint at this stage, which demonstrates flexural behaviour. Flexural action developed until the left bottom angle fractured close to the heel at a displacement of 260 mm. There was a dip followed by a rise in the reaction–displacement curve in Fig. 11a until fracture of the right bottom angle occurred. It is noteworthy that catenary action was partially mobilised after fracture of the left bottom angle. Fig. 11 shows that at the stage of catenary action, large tensile forces developed in the beams and the bending moments reversed in sign since the moment calculations were based on the beam neutral axis. Due to limited tying capacity at the second stage, the applied load could not exceed the peak load attained at the first stage. With regard to the capacity to form large deformation and catenary action, this connection has relatively limited rotation capacity compared to the web cleat connection. As shown in Fig. 12 and Table 2, catenary action could not be fully mobilised and the maximum load was controlled by flexure rather than catenary action.

### 3.1.3. Specimen 3—TSWA (8 mm angle)

The TSWA (8 mm angle) connection has a similar behaviour in load and deformation capacities with the web cleat connection, as shown in Fig. 13 and Table 2. With regard to the force–displacement history shown in Fig. 13, there is no obvious point of demarcation between flexural and tensile phases The end of flexural action corresponds to the fracture of left bottom angle, as shown in Fig. 13c at a displacement of 230 mm, but the onset of catenary action is defined at the instant when the beam axial force shows tension, as indicated in Fig. 13b. In Fig. 13a, the two bottom angles fractured first, after which load continued to increase to the maximum value until one of the right web angles fractured at a displacement of 366.4 mm. Ultimately, the other right web angle also fractured. When the two bottom angles fractured, bending moment could not be sustained by the joint, which indicates the end of flexural action stage, as shown in Fig. 13c. Different from Specimen 2, compression was not observed in the beams. Instead, a significant tensile force formed in the beams before the fracture of bottom angles, which means catenary action co-existed with flexural action when vertical displacement ranged between 100 mm and 230 mm. As shown in Fig. 14, the same fracture pattern of web angles with the web cleat connection in Fig. 10 is

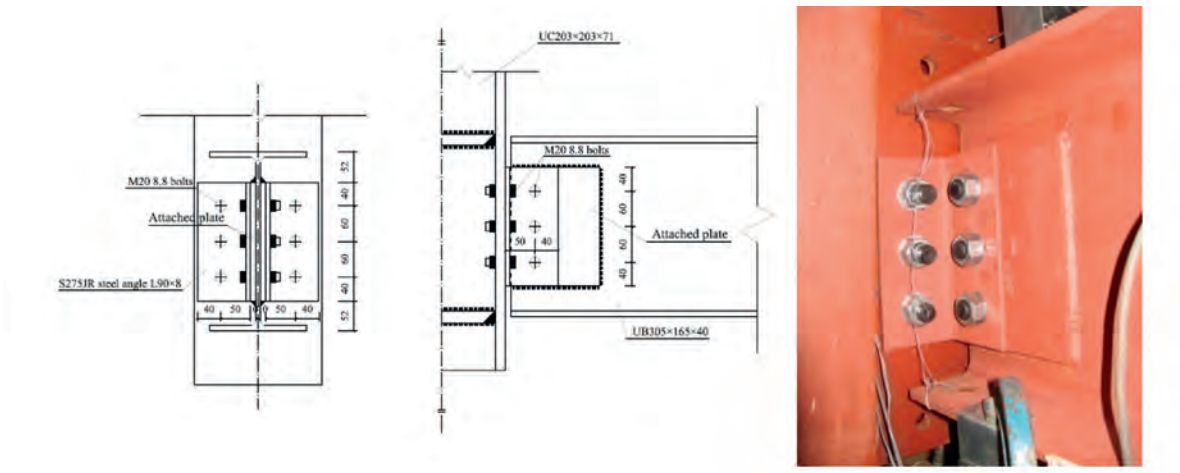


(a) Specimen 1 (web cleat)

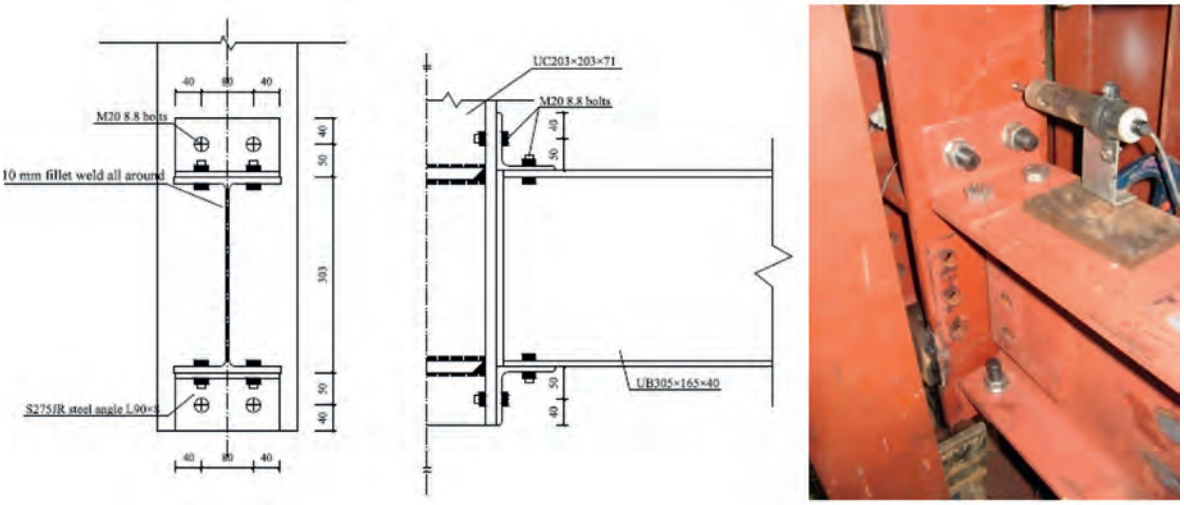


(b) Specimen 2 (top and seat)

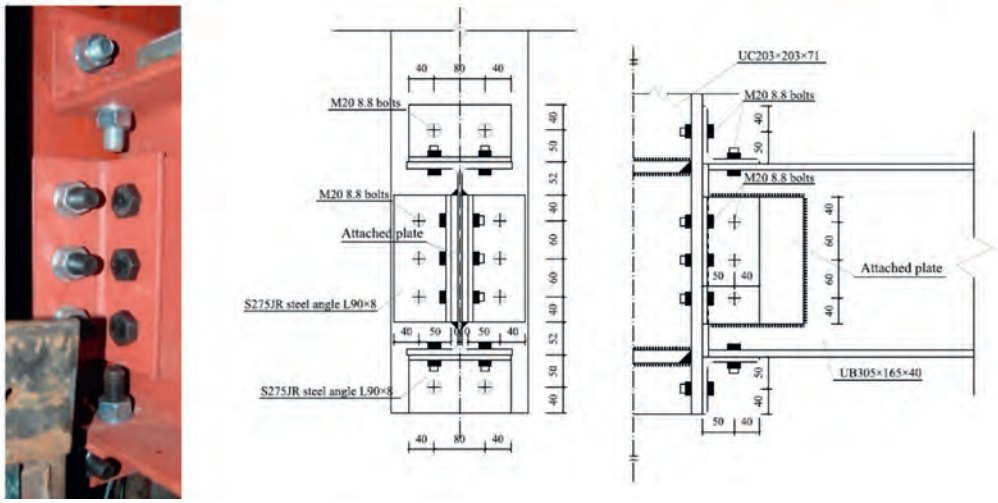


(c) Specimen 3 (TSWA-8mm angle)

**Fig. 8.** Details of test specimens (unit: mm).

observed. From Table 2, it can be concluded that Specimen 1 and Specimen 3 have attained almost the same load and rotation capacities and axial force in connecting beams.

*3.1.4. Specimen 4—fin plate*

Compared with the web cleat connection, the fin plate connection has a smaller rotation capacity. As shown in Figs. 15 and 16,

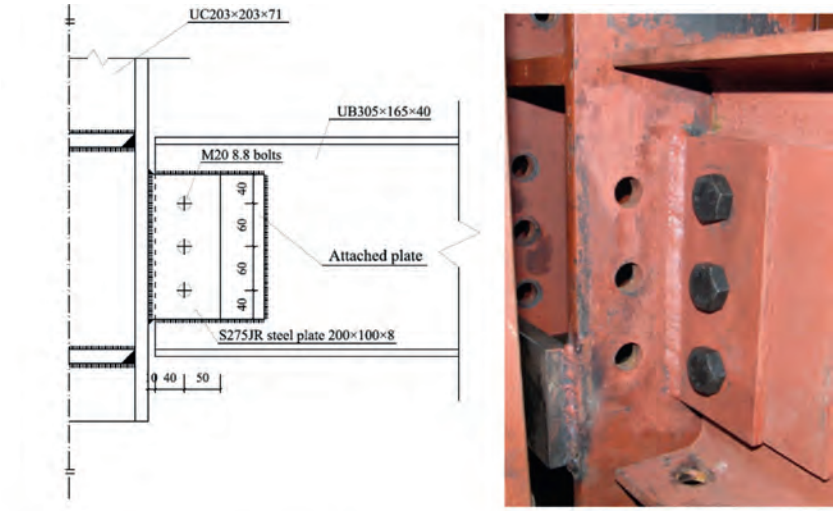


(d) Specimen 4 (fin plate)

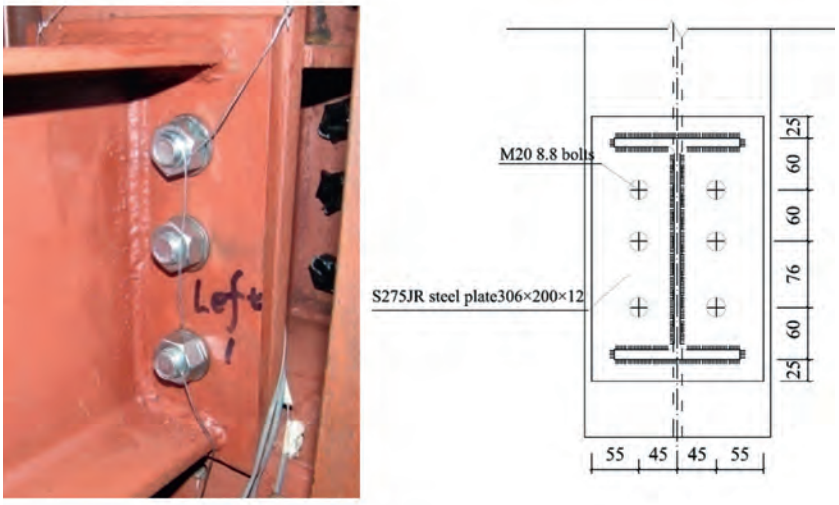


(e) Specimen 5 (flush end plate)

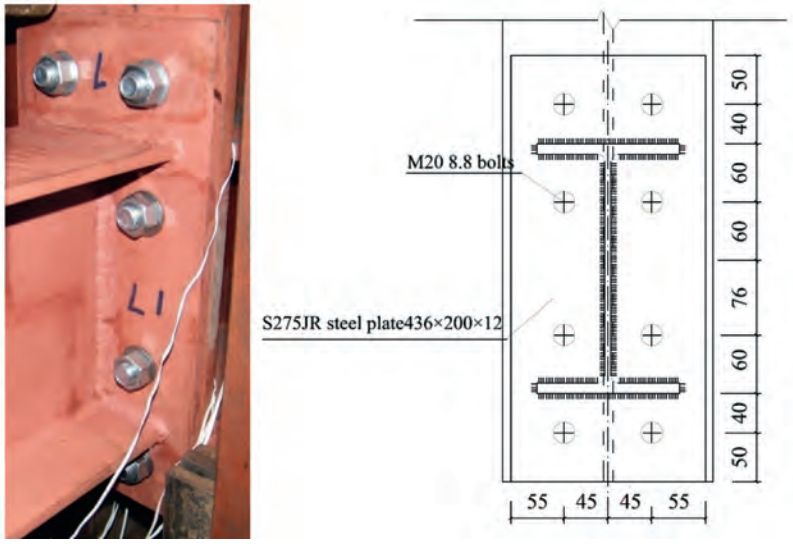


(f) Specimen 6 (extended end plate)

**Fig. 8.** (*continued*)

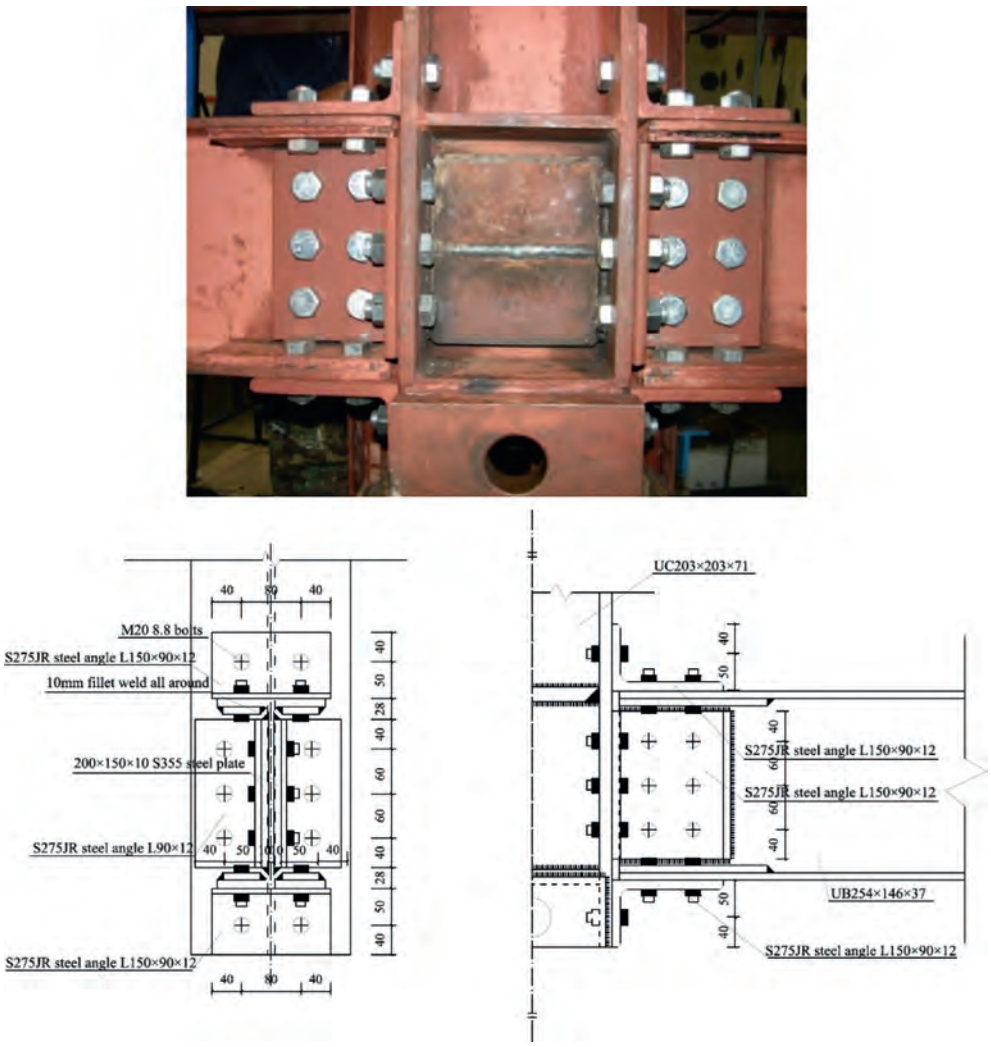


(g) Specimen 7 (TSWA-12mm angle)

**Fig. 8.** (*continued*)

this connection failed by shear fracture of bolts. The three bolts at the left connection failed one by one but there was no fracture of bolts at the right connection. At failure, the fin plate has undergone significant bearing deformations around the bolt holes. As a typical example of a simple connection, at the initial loading stage, this connection could not sustain any load until flexural and catenary actions formed at the large deflection stage. To be different with the web cleat connection, this connection has a greater bending moment resistance. However, due to limited rotation capacity of this connection, it has low capacity against vertical load.

*3.1.5. Comparison of the simple connections*

Table 3 shows that, if catenary action is considered under a middle column-removal scenario, load capacity could increase significantly, especially for Specimens 1, 3 and 4. If only flexural action was considered, and if there was no horizontal restraint in the experimental tests, Specimens 1 and 4 could only sustain limited vertical loads due to their poor moment resistances. When catenary action is mobilised, large increase of load capacity is observed. Therefore, catenary action plays an important role for beam–column joints under the middle column-removal scenario, in which sufficient horizontal restraints is provided by surrounding structural elements. It should be mentioned that the load capacities of beam–column joints without catenary action are calculated based on the bending moments measured in the steel beams. Although these are calculated values, there should be little difference with actual tests, particularly so as the connections achieved maximum moments at small displacement, with little tension developed in the beams.

The responses of simple connections subjected to catenary action are compared in Table 3. It is clear from Tables 2 and 3 that Specimen 1 (web cleat) has the best performance in the development of catenary action as it attains the largest vertical displacement. This type of connection could resist the highest vertical load, generate the largest vertical displacement and joint rotation, as it has the highest rotation capacity in the group of simple connections. Another observation from Table 2 is that, the horizontal reaction of Specimen 1 (web cleat) is slightly less than Specimen 4 (fin plate) although the vertical load capacity of the web cleat connection is much higher. This relatively low horizontal reaction could place a lower demand on adjacent columns. Specimen 3 has a similar behaviour in load and deformation capacities with Specimen 1 although this joint used up more angles and bolts. At the first stage, this specimen sustained a much higher load than Specimen 1 due to its higher flexural stiffness. However, when bottom angles fractured, similar vertical load and axial force curves were observed in these two tests, which means the top angles were not effective at catenary action stage. Specimen 4 formed large tensile forces in beams, but due to its lim-

**Table 2**
List of test results.

| Specimen ID | Connection type | | Maximum vertical load (kN) | Displacement[a] (mm) | Joint rotation[b] (deg) | Maximum horizontal reaction (kN) | Maximum moment (kN m) | Maximum axial fore of the beam, *F* (kN) | Failure mode |
|---|---|---|---|---|---|---|---|---|---|
| Specimen 1 | Simple connections | Web cleat | 119 | 367 | 8.97 | 349 | 5.9 | 369 | Angle fracture |
| Specimen 2 | | Top and seat angle | 44.8 | 243 | 5.96 | 115 | 49.8 | 120 | Angle fracture |
| Specimen 3 | | TSWA (8 mm angle) | 113 | 366.4 | 8.95 | 376 | 60.3 | 380.5 | Angle fracture |
| Specimen 4 | | Fin plate | 77.5 | 227 | 5.57 | 363 | 10.3 | 365 | Bolt fracture in shear |
| Specimen 5 | Semi-rigid connections | Flush end plate | 161.1 | 350 | 8.56 | 567 | 79.2 | 574 | Bolt thread stripping |
| Specimen 6 | | Extended end plate | 125.6 | 142 | 3.49 | 405.6 | 143.5 | 412.8 | Weld fracture |
| Specimen 7 | | TSWA (12 mm angle) | 229.8 | 398 | 9.71 | 670.7 | 91.4 | 680.4 | Bolt fracture |

[a] Displacement corresponding to the maximum load.
[b] Joint rotation corresponding to the maximum load.

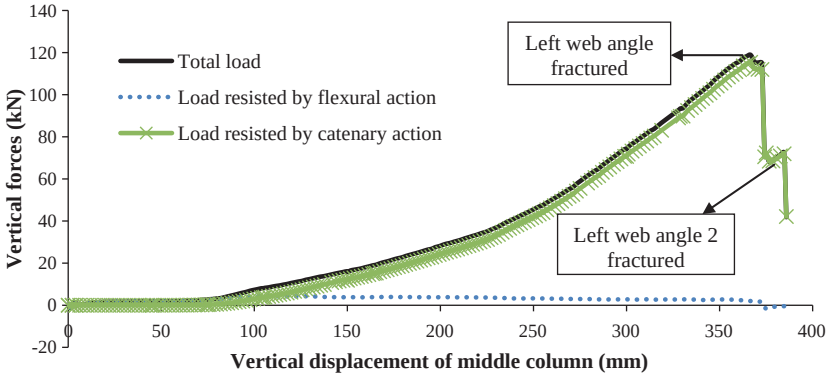


**Fig. 9.** Vertical force–middle column displacement curve of Specimen 1 (web cleat).

(a) Left web angle 1

(b) Left web angle 2

(c) Fractured angle

**Fig. 10.** Failure mode of Specimen 1 (web cleat).

ited rotation capacity, it had a low vertical load resistance. Specimen 2 has the poorest performance under catenary action. Hence, Specimen 1 (web cleat) has the best performance in resisting vertical loads. These benefits are due to its large rotation capacity, which could in turn mobilise catenary action.

### 3.2. Semi-rigid connections

#### 3.2.1. Specimen 5—flush end plate

As shown in Fig. 17, the force–displacement history can be divided into two stages: flexural action and catenary action. After local buckling of the top flange of the left beam, flexural moment decreased gradually and then the bottom bolt-row failed by thread stripping. Finally, failure propagated to the top two bolt-rows and subsequently, the left connection was completely severed. It should be noted that flush end plate connection is a typical type of semi-rigid connection, and therefore at the initial loading stage, vertical load increased due to its high flexural stiffness. After local buckling of the top beam flange, applied load could not increase any more until catenary action kicked in and resisted the vertical load. Thread stripping failure of top bolt-row shown in Fig. 18b defines the ultimate capacity for this connection. Although this type of joint finally failed due to thread stripping of bolts, as shown in Fig. 18, large displacement has developed due to significant bending of the end plate before failure.

Fig. 19 depicts the displacement profiles of the beams at different load levels. It shows that before plastic hinge formation, the whole specimen deflected like a simply-supported beam. After local buckling had occurred, a slight middle column rotation was observed and plastic hinge became more pronounced in the deflection profiles. Beyond 69.9 kN, the displacement profile of

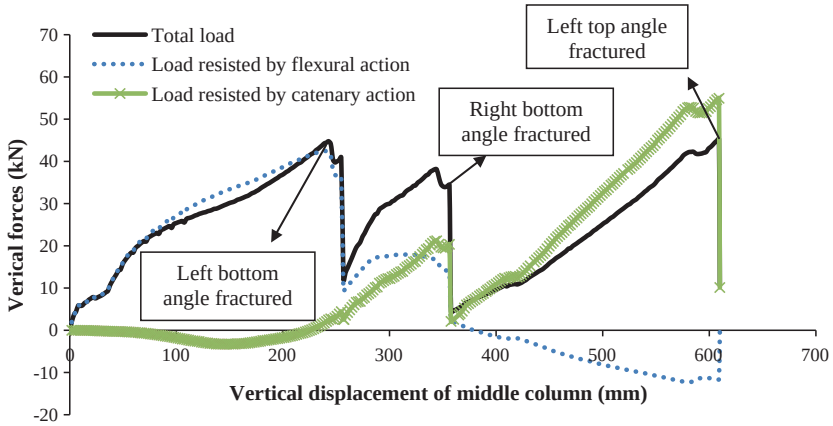


(a) Vertical force-middle column displacement curve

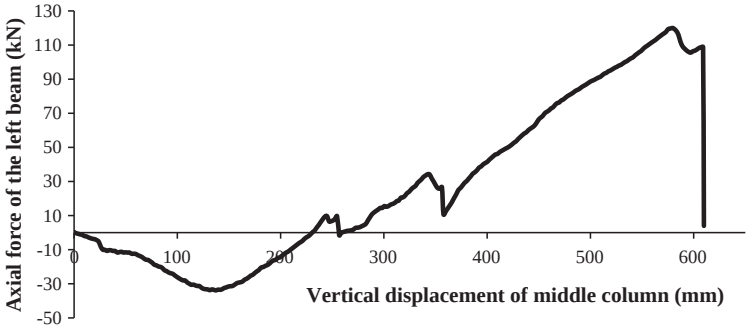


(b) Left beam axial force-middle column displacement curve

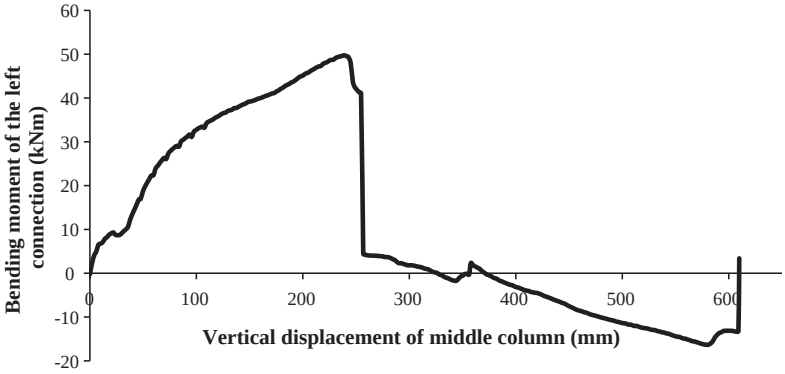


(c) Left connection moment-middle column displacement curve

**Fig. 11.** Action–middle column displacement curve of Specimen 2 (top and seat angle).

(a) Failed connection (b) Fractured left bottom angle

**Fig. 12.** Failure mode of Specimen 2 (top and seat angle).

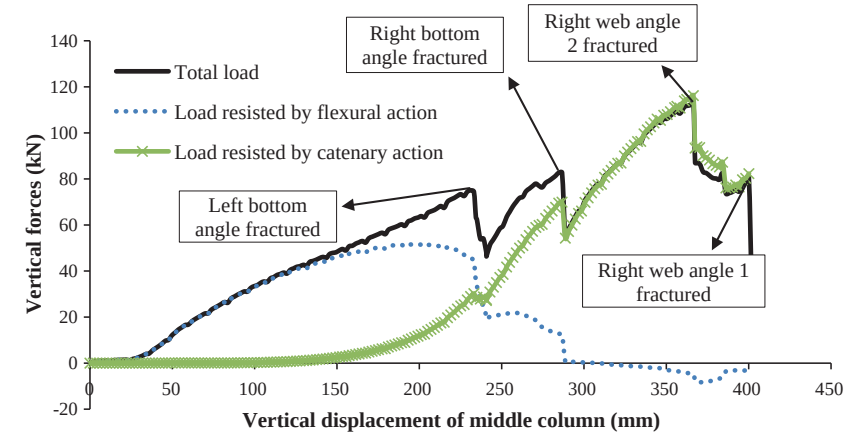


(a) Vertical force-middle column displacement curve

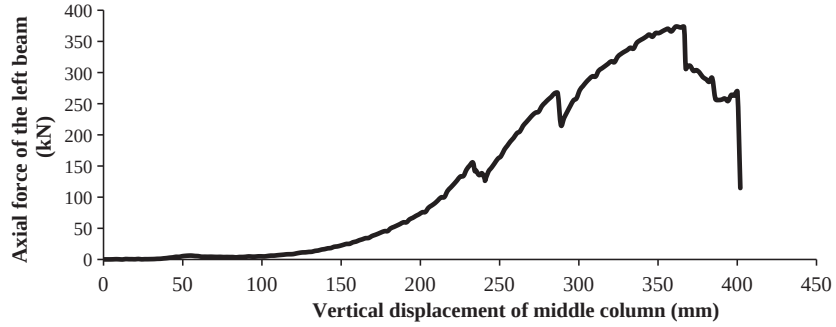


(b) Left beam axial force-middle column displacement curve

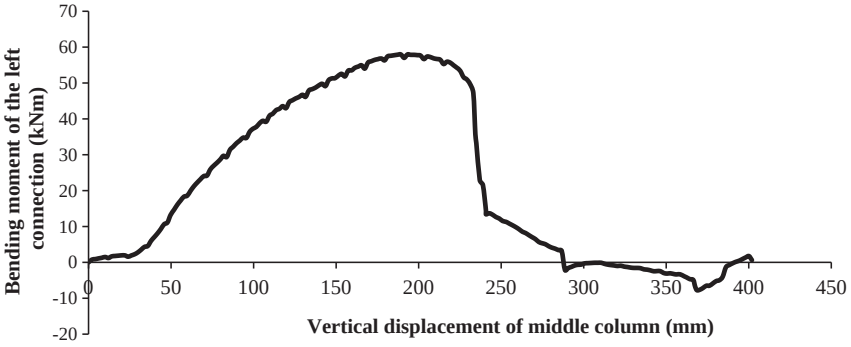


(c) Left connection moment-middle column displacement curve

**Fig. 13.** Action–middle column displacement curve of Specimen 3 (TSWA-8 mm angle).

each beam can be approximated by a straight line, which indicates the formation of plastic hinges at the beam–column connections.

*3.2.2. Specimen 6—extended end plate*

Fig. 20 shows the force–displacement history of Specimen 6. Extended end plate connection has the greatest flexural stiffness and moment strength among these seven specimens. Under normal loads, the top beam flange is under tension while the bottom beam flange is in compression. However, under column-removal scenarios, the moment reversed in sign. Therefore, the original compression zone is under tension. Partial-strength weld was used in the original compression zone, viz. bottom beam flanges. Hence, under positive bending moment, the bottom flange partial-strength weld at the right connection sustained a large tensile force and fractured first, as shown in Fig. 21. After that, there was a drop in the applied load. It should be noted that the middle column rotated due to unbalanced flexural actions at two sides of the joint. Ultimately, the specimen failed completely due to bolt thread stripping failure at the left connection, as shown in Fig. 21. This connection sustained substantial bending moment at the initial loading stage whereas at the large displacement stage, there was no further increase of loading in catenary action, unlike the flush end plate case.

*3.2.3. Specimen 7—TSWA (12 mm angle)*

In the test of Specimen 7, as shown in Fig. 22, there is no obvious point of demarcation between flexural and tensile phases. Fig. 22 shows that load could increase significantly before the two bottom bolts at the left connection fractured. Then the two bottom bolts at the right connection fractured, after which the load increased to the maximum value until the bolts connecting the web angles started to fracture one by one at a displacement of 398 mm. As shown in Fig. 23b, a 45° full-slant fracture surface indicates that

(a) Failed connection (b) Fractured web angle

**Fig. 14.** Failure mode of Specimen 3 (TSWA-8 mm angle).

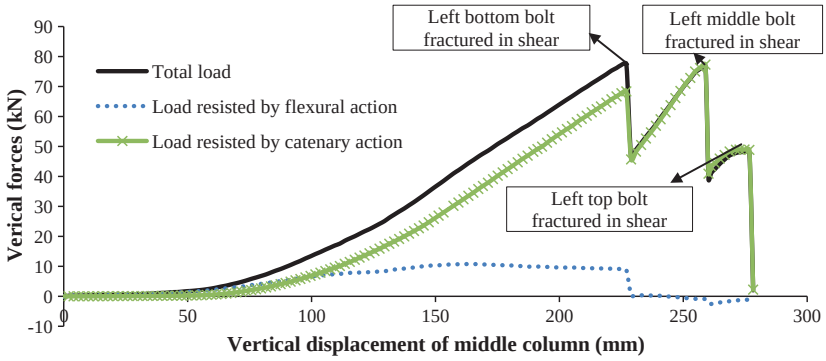


**Fig. 15.** Action–middle column displacement curve of Specimen 4 (fin plate).

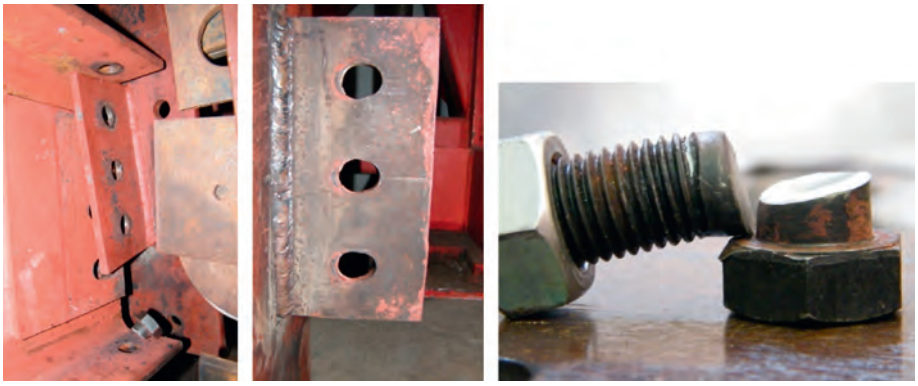

(a) Failed connection (b) Deformation of fin plate (c) Bolt fractured in shear

**Fig. 16.** Failure mode of Specimen 4 (fin plate).

the bolts were in tension as well as in shear. Although this specimen failed by bolt fracture, the rotation capacity (9.71°) is still higher than Specimen 3 (8.95°). This is due to a higher span-beam depth ratio (9.1) of this specimen compared with Specimen 3 (7.33). This conclusion demonstrates that for TSWA connections, span-beam depth ratio has a great influence on joint rotation capacity.

*3.2.4. Comparison of the semi-rigid connections*

Table 3 shows for semi-rigid beam–column joints, if catenary action is considered under a middle column-removal scenario, the load capacities could increase significantly, especially for Specimens 5 and 7. If only flexural action is considered, Specimen 6 could still achieve its load capacity, which indicates that catenary

**Table 3**
Comparison with and without catenary action.

| Specimen ID | Connection type | | Load capacity considering catenary action (kN) | Load capacity without catenary action[a] (kN) | Load capacity increase caused by catenary action (%) |
|---|---|---|---|---|---|
| Specimen 1 | Simple connections | Web cleat | 119 | 4.46 | 2568 |
| Specimen 2 | | Top and seat angle | 44.8 | 42.53 | 5 |
| Specimen 3 | | TSWA (8 mm angle) | 113 | 51.64 | 119 |
| Specimen 4 | | Fin plate | 77.5 | 10.78 | 619 |
| Specimen 5 | Semi-rigid connections | Flush end plate | 161.1 | 74.16 | 117 |
| Specimen 6 | | Extended end plate | 125.6 | 122.86 | 2 |
| Specimen 7 | | TSWA (12 mm angle) | 229.8 | 78.32 | 193 |

[a] The load capacities without catenary action are calculated based on the maximum moments of joints listed in Table 2.

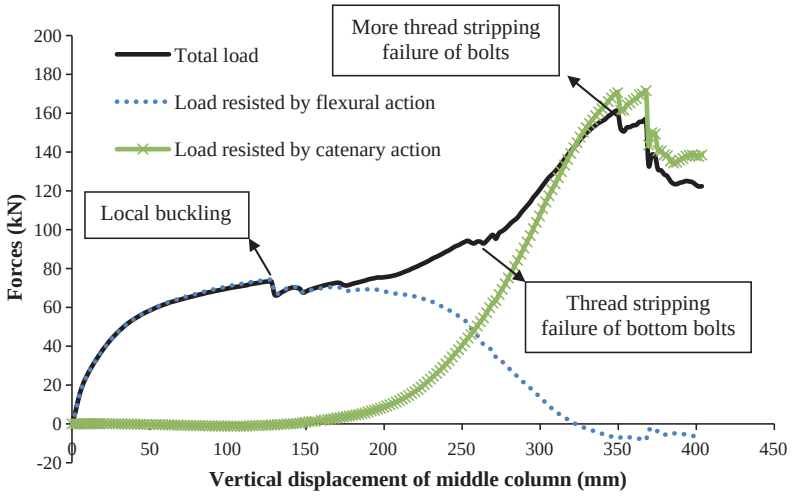


**Fig. 17.** Vertical force–middle column displacement curve of Specimen 5 (flush end plate).

(a) Failed connection (b) Bolt thread stripping

**Fig. 18.** Failure mode of Specimen 5 (flush end plate).

action has little influence on this joint. In contrast, under catenary action the load resistances of Specimens 5 and 7 could increase more than 100% of their capacities without catenary action.

The responses of the semi-rigid connections subjected to catenary action are compared in Table 3 and Fig. 24. The steel beam–column joints in these three tests went through two phases. During the first stage, the joints sustained vertical applied loads by flexural action. Specimen 6 has the greatest flexural strength. Therefore, at this stage, this specimen reached the largest loads among these three tests, as shown in Fig. 24b. At the second stage when the deflection was very large, the specimens went into catenary action. Specimens 5 (flush end plate) and 7 (TSWA-12 mm) performed well under catenary action. Fig. 24a shows that at the stage of flexural action, no axial forces were developed in beams and at the second stage (catenary action), tensile forces formed rapidly. Among these three tests, Specimen 7 had the largest load and rotation capacities. In the tests of Specimens 5 and 7, although finally the failure modes are due to bolt fracture or bolt thread stripping, there was a ductile failure process. Before failure of bolts, end plate or angles yielded and experienced high local plastic deformation

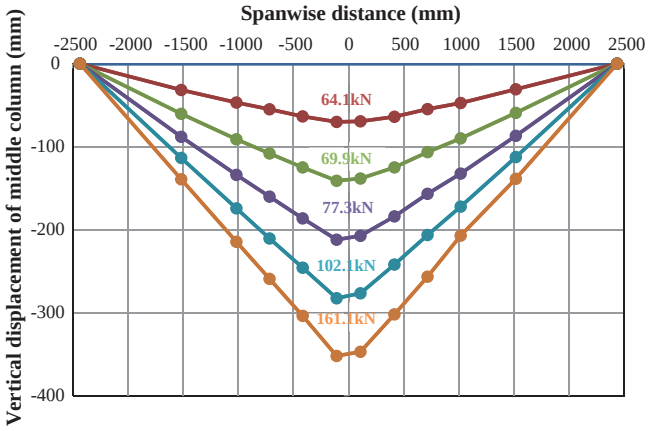


**Fig. 19.** Middle column displacement profiles of beams corresponding to indicated vertical forces for Specimen 5 (flush end plate).

and rotation, which introduced plastic hinges into the beam–column joints and consequently mobilised catenary action. Nevertheless, brittle failure was observed in Specimen 6 and this failure mode severely limited the formation of catenary action.

## 4. Practical implications of the experimental results

The experimental results demonstrate that under a middle column-removal scenario, beam–column joints sustain a combination of shear, tensile forces and bending moments. However according to the measured internal forces of beams at the maximum load values, for those joints which could develop catenary action well, tensile forces usually dominate the behaviour and the failure modes of joints. The behaviour of Specimens 1, 3, 4, 5 and 7, which could form catenary action well, is analogous to a truss system, as shown in Fig. 25. In this system, rotation value $\theta$ and tensile resistance of connection $T$ are obtained from the experimental results and the applied load $P$ can be calculated based on equilibrium:

$$P = 2T \sin\theta \tag{1}$$

The comparison between the experimental and calculated results is shown in Table 4. Clearly, the calculated values agree very well with the test results with a mean of 99.8% and a small standard deviation of 6%. This indicates that after large rotations have occurred, beam–column joints are subjected to pure tension and tensile failure controls the final failure modes of these joints.

In the experimental programme, only one test was conducted for each type of connections. In order to consider other connection configurations, such as different number of bolts and different

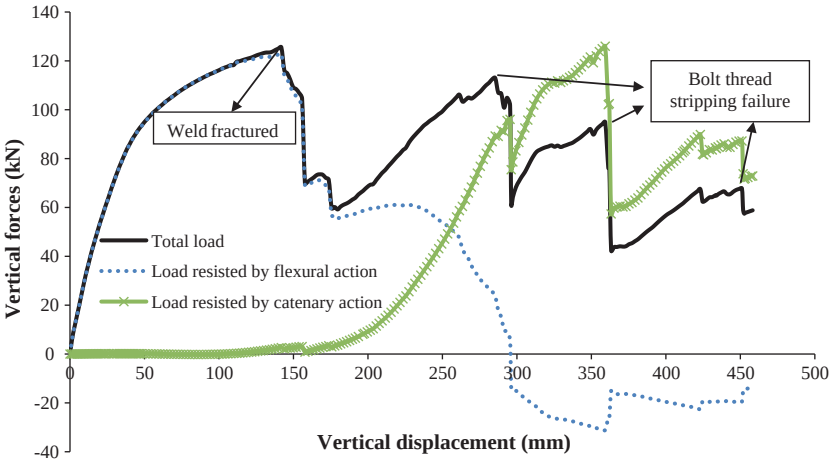


**Fig. 20.** Vertical force–middle column displacement curve of Specimen 6 (extended end plate).

(a) Failed connection (b) Fracture of weld

**Fig. 21.** Failure mode of Specimen 6 (extended end plate).

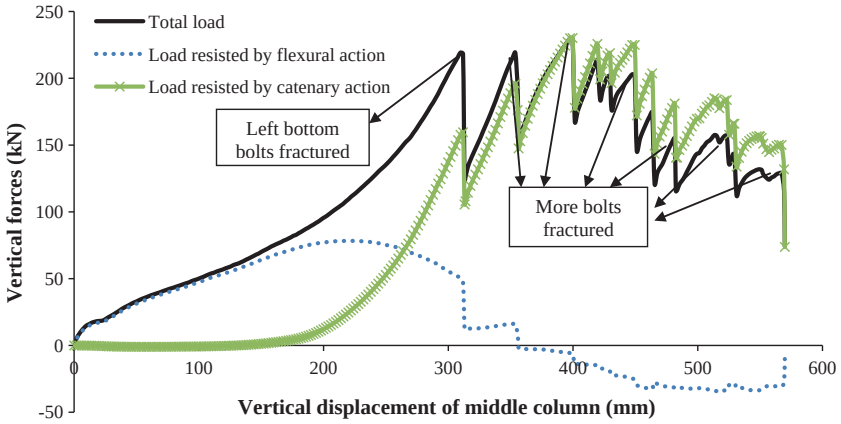


**Fig. 22.** Vertical force–middle column displacement curve of Specimen 7 (TSWA-12 mm angle).

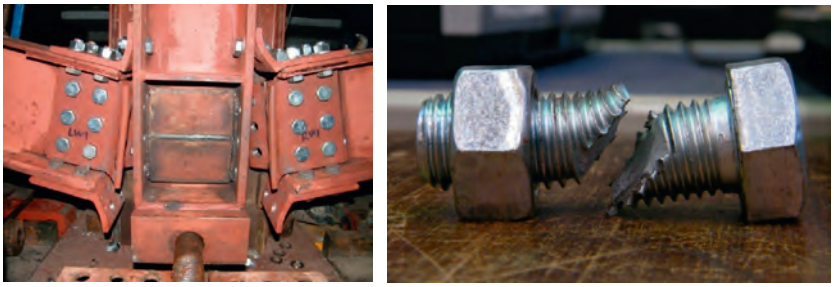

(a) Failed connection (b) Fracture bolt

**Fig. 23.** Failure mode of Specimen 7 (TSWA-12 mm angle): (a) failed connection and (b) fracture bolt.

beam section depth, a series of numerical simulations have been conducted by Yang and Tan [24]. These numerical models were validated by the beam–column joint tests, which have been presented in this paper. In addition, an extensive parametric study was undertaken using these validated models to obtain the rotation capacities of various types of connections under catenary action. The work [24] shows that current acceptance criteria of rotation capacities for steel joints such as web cleat, fin plate, flush end plate and TSWA connections, are probably too conservative as they only consider pure flexural resistance. Finally, some practical design implications have been drawn up from the parametric study and four new connection acceptance criteria of rotation capacities have been proposed to consider catenary action under a middle column removal scenario. These connection acceptance criteria could be used in Eq. (1) to calculate the load resistances of connections under catenary action.

Table 5 indicates a comparison of tying resistance between the design values from Table 1 and the test results from Table 2. From Table 5, it can be concluded that certain types of connections could not develop the designed tying capacities based on Eurocode 3 [3] and BCSA/SCI [30]. In the design stage, only pure shear or pure tying forces are considered, whereas under column-removal scenarios beam–column joints sustain pure tensile forces *after undergoing large rotations*, which means the load resistances of beam–column joints are related to tying resistances as well as rotation capacities. This implies that when tying capacity design method [34] is used to mitigate progressive collapse, tying resistances of beam–column joints should still satisfy certain values after large rotations have occurred. Therefore, enhancing tensile resistances of beam–column joints *after undergoing large rotations* is one of the most effective means to mitigate progressive collapse. In current Eurocode 1 [34], only tying force magnitudes are required. However, the beam–column joints may not have the required rotation capacity to develop catenary action. Thus, certain types of joints have failed to achieve the design tying resistance, as shown in Table 5 (Specimens 2 and 6). It should also be mentioned that although the design tying resistances of Specimens 3, 5 and 7 have been met in the experiments, the ratios of $P_T/P_D$ exceed unity by a relatively small margin compared to those of Specimens 1 and 4. Therefore, for these types of connections, the influence of rotations should be considered in the design stage.

Based on the discussion, Eq. (2) is proposed to replace the expression of tying resistance in the design code [34]:

$$T' = T\sin\theta \tag{2}$$

where $T'$ is the tying requirements in Eurocode 1 [34], $T$ is beam–column joint tensile resistance after undergoing rotation $\theta$, and $\theta$ is the rotation capacity of connection.

Table 5 also summarizes the rotation capacities based on the tests conducted in this study and on the recommended values by DoD [2] and ASCE [35]. The design values of the rotation capacities are obtained from Table 5-2 [2] and Table 5-6 [35], as well as the failure modes observed in the tests. As Table 5 indicates, the rotations at peak loads based on the experimental results in this study were much higher than the recommended values by DoD [2] and ASCE [35]. In the current design codes [1,2] against progressive collapse, there are no experimental results available for bolted steel beam–column joints, and the recommended values are based on seismic testing data. However, under a middle column-removal scenario, connections sustain monotonic loads rather than seismic actions. Under seismic loading, the connections are under pure flexure and cyclic loading leading to significant degradation in the strength and ductility. In contrast, under catenary action, the connections are subjected to pure tension after undergoing large

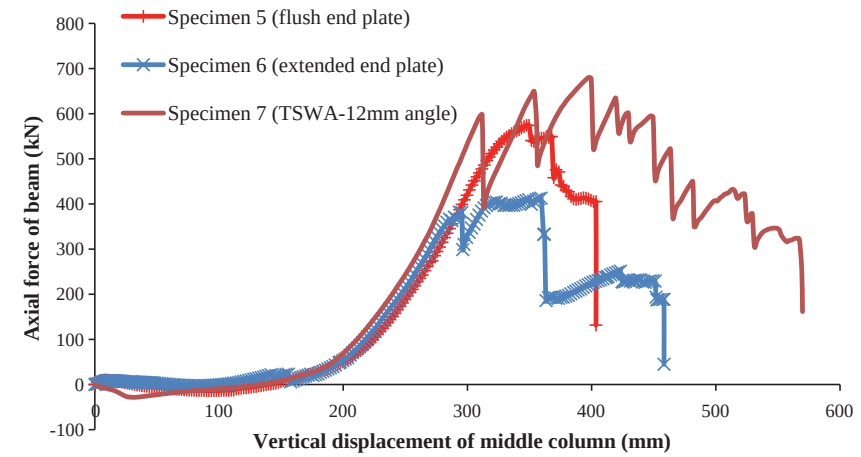


(a) Beam axial force-middle column displacement curves

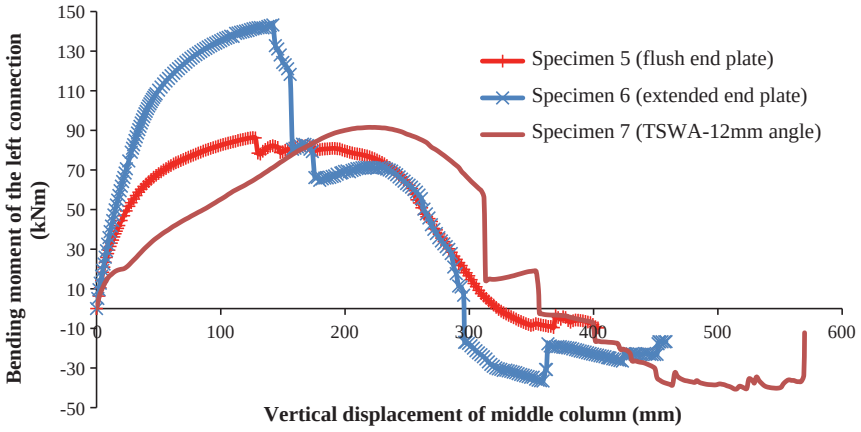


(b) Connection moment-middle column displacement curves

**Fig. 24.** Comparison of the behaviour of different semi-rigid connections.

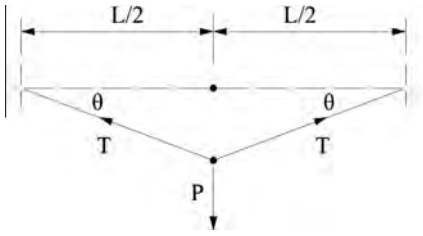


**Fig. 25.** Simplified truss system.

**Table 4**
Comparison between experimental results and calculated values based on the simplified models.

| Specimen ID | Load capacity from experimental results, $P_E$ (kN) | Load capacity from calculated values, $P_C$ (kN) | $P_C/P_E$ (%) |
|---|---|---|---|
| Specimen 1 | 119 | 115.1 | 96.7 |
| Specimen 3 | 113 | 118.4 | 104.8 |
| Specimen 4 | 77.5 | 70.9 | 91.5 |
| Specimen 5 | 161.1 | 170.9 | 106.1 |
| Specimen 7 | 229.8 | 229.5 | 99.9 |

Mean $P_C/P_E$ = 99.8%.
Standard deviation $P_C/P_E$ = 0.06.

rotations. Hence, seismic testing data may not be appropriate for column-removal scenarios.

It should be mentioned that in this paper, only one test for each type of connections was conducted. However, even for the same type of connections, if the connection configurations like number of bolts, bolt size and plate or angle thickness, are changed, the structural behaviour will be changed. Based on the experimental data presented in this paper, Yang and Tan [24] conducted further numerical simulations to investigate the effects of different number of bolts and different beam section depth. Yang and Tan [36] conducted further experimental tests for bolted angle connections in order to investigate the effect of angle thickness. However, it may also necessary to study the effects of bolt size, plate thickness and other connection configuration parameters for fin plate and end plate connections.

## 5. Summary and conclusions

This paper presents the descriptions and experimental results of seven tests on steel beam–column joints subjected to catenary action. The following conclusions can be drawn:

(1) The test specimens revealed various modes of fracture in the connection regions, ductility of different failure modes and rotation capacities of various types of connections under a middle column-removal scenario.

**Table 5**
Comparison of tying resistances and rotation capacities of beam–column joints between the design values and the test results.

| Specimen ID | Connection type | | Tying resistances | | | Rotation capacities (degree) | |
|---|---|---|---|---|---|---|---|
| | | | Design values, $P_D$ (kN) | Test results, $P_T$ (kN) | $P_T/P_D$ | Design values [2,8] | Test results |
| Specimen 1 | Simple connections | Web cleat | 177 | 369 | 2.08 | 5.71 | 8.97 |
| Specimen 2 | | Top and seat angle | 153 | 120 | 0.78 | 2.01 | 5.96 |
| Specimen 3 | | TSWA (8 mm angle) | 330 | 380.5 | 1.15 | 2.01 | 8.95 |
| Specimen 4 | | Fin plate | 198 | 365 | 1.84 | 2.47 | 5.57 |
| Specimen 5 | Semi-rigid connections | Flush end plate | 480 | 574 | 1.20 | 0.86 | 8.56 |
| Specimen 6 | | Extended end plate | 546 | 412.8 | 0.76 | 0.57 | 3.49 |
| Specimen 7 | | TSWA (12 mm angle) | 495 | 680.4 | 1.37 | 0.74 | 9.71 |

(2) The test results demonstrate the contribution of catenary action to the load resistances of various types of steel beam–column joints and conclude that under the middle column-removal scenario, catenary action can be considered to increase the load capacity.
(3) For web cleat and fin plate connections, under the middle column-removal scenario, only a limited load could be applied onto the joints at the initial loading stage and the applied load increased significantly at the large deformation stage due to catenary action. Therefore, the behaviour of these two joints was dominated by catenary action. For top and seat angle and extended end plate connections, flexural action dominates the behaviour of the joints in the early stage of the response. There was little load contribution from catenary action. For flush end plate and TSWA (8 mm and 12 mm angle) connections, significant flexural actions were observed and catenary action could also develop well at large deformation stage.
(4) In the group of simple connections, the web cleat connection has the best combination of desirable features: ability to develop catenary action and extremely high ductility (rotational capacity) through deformation of the web angles. The TSWA (8 mm angle) connection has a similar behaviour with the web cleat connection. In the group of semi-rigid connections, TSWA (12 mm angle) achieved the highest load and rotation capacities whereas flush end plate could also mobilize catenary action well.
(5) By comparing Specimens 3 and 7, it can be seen that for the connection type of TSWA, span-beam depth ratio has a great influence on the rotation capacities of connections.
(6) It is worthy to note that tensile capacities of beam–column joints after undergoing large rotations usually control the failure mode and the formation of catenary action. This implies that engineers should adopt high tensile resistances of beam–column joints after undergoing large rotations rather than pure tying resistance. A new tying resistance expression is proposed to consider the effect of large rotation. If large rotation is not considered in the design stage, the joints with poor rotation capacities would fail to achieve the design tying resistances.
(7) The rotations of beam–column joints at peak loads based on the experimental results in this study were much higher than the recommended values by DoD [2] and ASCE [35].

## References


[1] General Services Administration (GSA). Progressive collapse analysis and design guidelines for new federal office buildings and major modernization projects, Washington, DC; 2003.
[2] Department of Defense (DoD). Design of buildings to resist progressive collapse, unified facilities criteria, 4-023-03; 2009.
[3] European committee for standardization. Eurocode 3: design of steel structures—Part 1-8: design of joints, BS EN 1993-1-8:2005. British Standards Institution, UK; 2005.
[4] Khandelwal K, El-Tawil S. Collapse behaviour of steel special moment resisting frame connections. J Struct Eng – ASCE 2007;133(5):646–55.
[5] Sadek F, Main JA, Lew HS, Robert SD, Chiarito V. Testing and analysis of steel beam–column assemblies under column removal scenarios. In: Proceedings of the 2009 structures congress, USA; 2009.
[6] Karns JE, Houghton DL, Hong JK, Kim J. Behaviour of varied steel frame connection types subjected to air blast, debris impact, and/or post-blast progressive collapse load conditions. In: Proceedings of the 2009 structures congress, USA; 2009.
[7] Demonceau JF. Steel and composite frames: sway response under conventional loading and development of membrane effects in beams further to an exceptional action. Doctor of Philosophy thesis. Civil and Environmental Engineering, University of Liège; 2008.
[8] Izzuddin BA, Vlassis AG, Elghazouli AY, Nethercot DA. Progressive collapse of multi-storey buildings due to sudden column loss. Part I: simplified assessment framework. Eng Struct 2008;30(5):1308–18.
[9] Vlassis AG, Izzuddin BA, Elghazouli AY, Nethercot DA. Progressive collapse of multi-storey buildings due to sudden column loss. Part II: application. Eng Struct 2008;30(5):1424–38.
[10] Qian K, Li B. Dynamic performance of RC beam–column substructures under the scenario of the loss of a corner column – experimental results. Eng Struct 2012;42:154–67.
[11] Sun RR, Huang ZH, Burgess IW. Progressive collapse analysis of steel structures under fire conditions. Eng Struct 2012;34:400–13.
[12] Khandelwal K, El-Tawil S. Pushdown resistance as a measure of robustness in progressive collapse analysis. Eng Struct 2011;33(9):2653–61.
[13] Xu GQ, Ellingwood BR. Disproportionate collapse performance of partially restrained steel frames with bolted T-stub connections. Eng Struct 2011;33(1):32–43.
[14] Bao YH, Kunnath SK. Simplified progressive collapse simulation of RC frame-wall structures. Eng Struct 2010;32(10):3153–62.
[15] Ding J, Wang YC. Experimental study of structural fire behaviour of steel beam to concrete filled tubular column assemblies with different types of joints. Eng Struct 2007;29(12):3485–502.
[16] Dai XH, Wang YC, Bailey CG. Numerical modelling of structural fire behaviour of restrained steel beam–column assemblies using typical joint types. Eng Struct 2010;32(2010):2337–51.
[17] Elsawaf S, Wang YC, Mandal P. Numerical modelling of restrained structural subassemblies of steel beam and CFT columns connected using reverse channels in fire. Eng Struct 2011;33:1217–31.
[18] Wang YC, Dai XH, Bailey CG. An experimental study of relative structural fire behaviour and robustness of different types of steel joint in restrained steel frames. J Constr Steel Res 2011;67(7):1149–63.
[19] Wang YC. Performance based fire engineering research of steel and composite structures: a review of joint behaviour. Adv Struct Eng 2011;14(4):613–24.
[20] Yu HX, Burgess IW, Davison JB, Plank RJ. Experimental investigation of the behaviour of flush plate connections in fire. In: Proceedings of the fifth international conference on structures in fire, Singapore; 2008.
[21] Yu HX, Burgess IW, Davison JB, Plank RJ. Experimental study on flexible end plate connections in fire. In: Proceedings of the fifth 5th European conference on steel and composite structures, Austria; 2008.
[22] Yu HX, Burgess IW, Davison JB, Plank RJ. Experimental investigation of the behaviour of fin plate connections in fire. J Constr Steel Res 2009;65(3):723–36.
[23] Yu HX, Burgess IW, Davison JB, Plank RJ. Tying capacity of web cleat connections in fire. Part 1: test and finite element simulation. Eng Struct 2009;31(3):651–63.
[24] Yang B, Tan KH. Numerical analyses of steel beam–column joints subjected to catenary action. J Constr Steel Res 2012;70:1–11.
[25] Yu J, Tan K-H. Experimental and numerical investigation on progressive collapse resistance of reinforced concrete beam column sub-assemblages. Eng Struct 2011. http://dx.doi.org/10.1016/j.engstruct.2011.08.040.
[26] Pham XD, Tan KH. Membrane actions of RC slabs in mitigating progressive collapse of building structures. Eng Struct 2011. http://dx.doi.org/10.1016/j.engstruct.2011.08.039.
[27] European committee for standardization. Eurocode 1—actions on structures—Part 1-1: general actions—densities, self-weight, imposed loads for buildings. BS EN 1991–1-1:2002. British Standards Institution, UK; 2002.

[28] European committee for standardization. Eurocode 3: design of steel structures—Part 1-1: general rules and rules for buildings, BS EN 1993-1-1:2005. British Standards Institution, UK; 2005.
[29] European committee for standardization. Eurocode 4: design of composite steel and concrete structures—Part 1-1: general rules and rules for buildings, BS EN 1994-1-1:2004. British Standards Institution, UK; 2004.
[30] BCSA/SCI. Joints in steel construction—simple connections. Steel Construction Institute, Ascot; 2002.
[31] BCSA/SCI. Joints in steel construction—moment connections. Steel Construction Institute, Ascot; 1995.
[32] BCSA/SCI. Joints in steel construction—composite connections. Steel Construction Institute, Ascot; 1998.
[33] AISC, American Institute of Steel Construction. Specification for structural steel buildings. AISC, Chicago, IL; 2005.
[34] European committee for standardization. Eurocode 1—actions on structures—Part 1-7: general actions—accidental actions, BS EN 1991-1-7:2006. British Standards Institution, UK; 2006.
[35] ASCE. Seismic rehabilitation of existing buildings (ASCE/SEI 41-06), Reston; 2006.
[36] Yang B, Tan KH. Robustness of bolted-angle connections against progressive collapse: experimental tests of beam–column joints and development of component-based models. J Struct Eng – ASCE 2012. http://dx.doi.org/10.1061/(ASCE)ST.1943-541X.0000749.